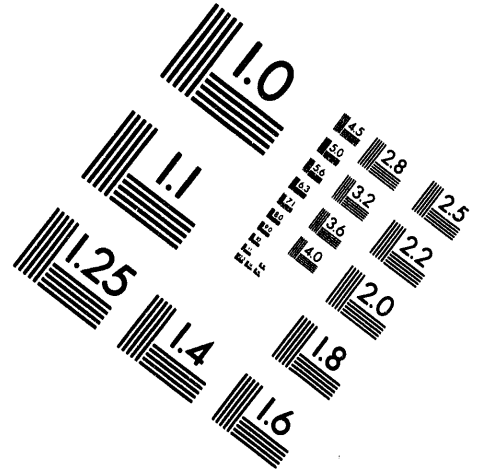
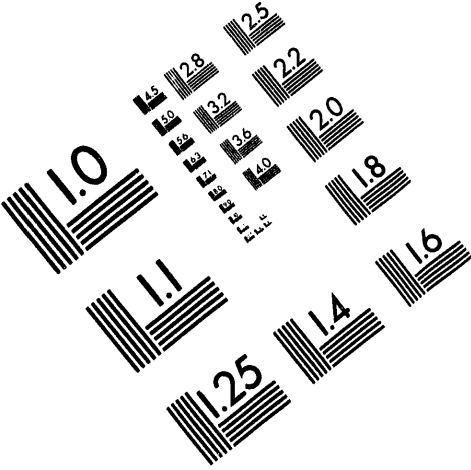




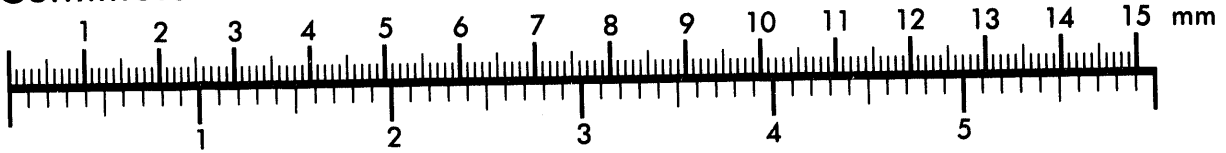
AIM

Association for Information and Image Management

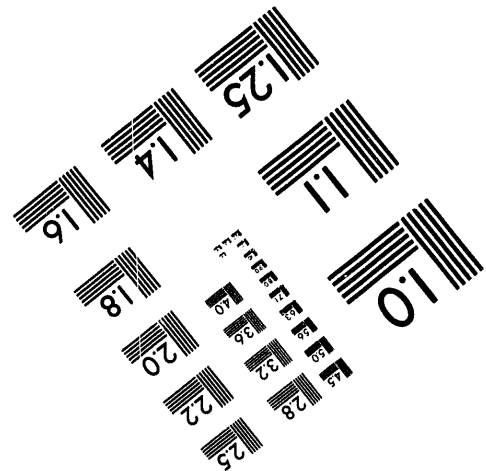
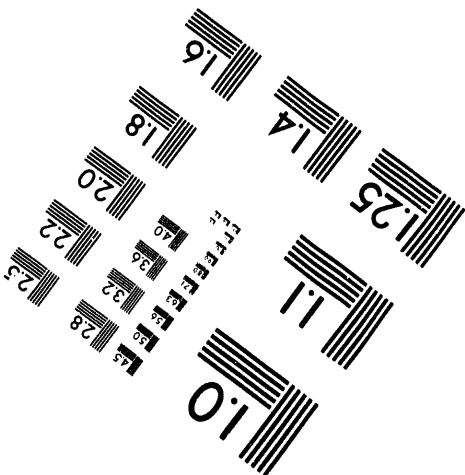
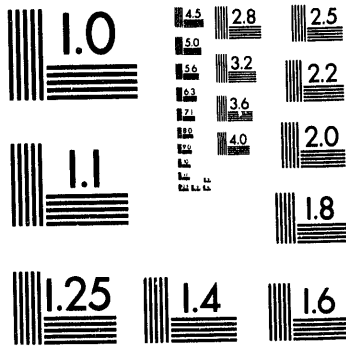
1100 Wayne Avenue, Suite 1100
Silver Spring, Maryland 20910
301/587-8202



Centimeter



Inches



MANUFACTURED TO AIM STANDARDS
BY APPLIED IMAGE, INC.

1

O

f

1

Interferometric Synthetic Aperture Radar Terrain Elevation Mapping from Multiple Observations

Dennis C. Ghiglia and Daniel E. Wahl
Sandia National Laboratories, Albuquerque,
New Mexico 87185

Abstract

All prior interferometric SAR imaging experiments to date dealt with pairwise processing. Simultaneous image collections from two antenna systems or two-pass single antenna collections are processed as interferometric pairs to extract corresponding pixel by pixel phase differences which encode terrain elevation height. The phase differences are wrapped values which must be unwrapped and scaled to yield terrain height. We propose two major classes of techniques that hold promise for robust multibaseline (multiple pair) interferometric SAR terrain elevation mapping. The first builds on the capability of a recently published method for robust weighted and unweighted least-squares phase unwrapping, while the second attacks the problem directly in a maximum likelihood (ML) formulation. We will provide several examples (actual and simulated SAR imagery) that illustrate the advantages and disadvantages of each method.

1.0 Introduction

SAR image collections can be processed in interferometric pairs to yield temporal change detection products or digital terrain elevation maps accurate in relative elevation to a few centimeters with accompanying spatial resolution dictated by the spatial res-

olution of the SAR images themselves [1]-[3]. No other previously developed terrain elevation mapping technology (such as optical stereoscopy) can yield maps with such precision, especially considering the day/night, all weather capability and long standoff distances possible with SAR.

All prior interferometric SAR imaging experiments to date dealt with pairwise processing. That is, simultaneous image collections from two antenna systems or two-pass single antenna collections are processed as interferometric pairs to extract corresponding pixel by pixel phase differences which encode terrain elevation height. The phase differences are wrapped values which must be unwrapped and scaled to yield terrain height. The phase-to-height scale factor is a function of the radar wavelength, imaging geometry, and baseline (i.e. effective antenna separation). With other parameters remaining fixed, larger baselines allow more accurate height estimation (and better height-to-phase noise ratios) but also increase the possibility of steep terrain causing phase aliasing, thereby destroying height measurements. On the other hand, small baselines reduce the possibility of phase aliasing but suffer from poorer phase noise performance and phase-to-height sensitivity. Clever processing of multiple collections could offer the advantages of large and small baselines. We propose two major classes of techniques that hold promise for robust multibaseline interferometric SAR terrain elevation mapping.

2.0 Least-Squares 2D Phase Unwrapping Method

This first class of methods builds on the capability of a recently published technique for robust weighted and unweighted least squares phase unwrapping [4]. This phase unwrapping method couches the problem in the solution of Poisson's equation with the interferometric pair data forming the measurements used in the PDE. It is easily shown that multibaseline data can be simply included (in a weighted or unweighted sense) in the

DISCLAIMER

This report was prepared as an account of work sponsored by an agency of the United States Government. Neither the United States Government nor any agency thereof, nor any of their employees, makes any warranty, express or implied, or assumes any legal liability or responsibility for the accuracy, completeness, or usefulness of any information, apparatus, product, or process disclosed, or represents that its use would not infringe privately owned rights. Reference herein to any specific commercial product, process, or service by trade name, trademark, manufacturer, or otherwise does not necessarily constitute or imply its endorsement, recommendation, or favoring by the United States Government or any agency thereof. The views and opinions of authors expressed herein do not necessarily state or reflect those of the United States Government or any agency thereof.

formation of the right hand side of Poisson's equation, which is then solved by the published techniques.

For example, consider the collection of a single pair of interferometric SAR images from which the wrapped pairwise phase data, $\psi_{i,j}$, are obtained. We wish to determine the unwrapped phase values $\phi_{i,j}$, at the same grid locations with the requirement that the spatial phase differences of the $\phi_{i,j}$ agree with those of the $\psi_{i,j}$ in the least-squares sense. To see how this is done, let us first define a wrapping operator W , that wraps all values of its argument into the range $(-\pi, \pi)$ by adding or subtracting an integral number of 2π radians from its argument. Therefore, for example, $W\{\phi_{i,j}\} = \psi_{i,j}$.

Next, we compute two sets of phase differences: those differences with respect to the i index, and those with respect to the j index. Specifically, from our known values of the wrapped phase $\psi_{i,j}$, we compute the following wrapped phase differences,

$$\Delta_{i,j}^x = W\{\psi_{i+1,j} - \psi_{i,j}\} \quad (\text{EQ 1})$$

$$i = 0 \dots M-2, \quad j = 0 \dots N-1$$

$$\Delta_{i,j}^x = 0, \text{ otherwise,}$$

and,

$$\Delta_{i,j}^y = W\{\psi_{i,j+1} - \psi_{i,j}\} \quad (\text{EQ 2})$$

$$i = 0 \dots M-1, \quad j = 0 \dots N-2$$

$$\Delta_{i,j}^y = 0, \text{ otherwise,}$$

where the x and y superscripts refer to differences in the i and j indices, respectively. The solution, $\phi_{i,j}$, that minimizes

$$\begin{aligned} \epsilon^2 = & \sum_{i=0}^{M-2} \sum_{j=0}^{N-1} \left(\phi_{i+1,j} - \phi_{i,j} - \Delta_{i,j}^x \right)^2 \\ & + \sum_{i=0}^{M-1} \sum_{j=0}^{N-2} \left(\phi_{i,j+1} - \phi_{i,j} - \Delta_{i,j}^y \right)^2 \end{aligned} \quad (\text{EQ 3})$$

is the least-squares solution.

It is shown in [4] that the solution of Poisson's equation on a rectangular M by N grid,

$$\frac{\partial^2}{\partial x^2} \phi(x, y) + \frac{\partial^2}{\partial y^2} \phi(x, y) = \rho(x, y) \quad (\text{EQ 4})$$

where,

$$\rho_{i,j} = \left(\Delta_{i,j}^x - \Delta_{i-1,j}^x \right) + \left(\Delta_{i,j}^y - \Delta_{i,j-1}^y \right), \quad (\text{EQ 5})$$

is the least-squares solution to the phase unwrapping problem.

We can incorporate k pairwise observations in the above formulation by solving (EQ 4) with a new right hand side, $\bar{\rho}$, that incorporates appropriate pairwise observations with associated scale factor equalizations in a weighted linear combination as,

$$\bar{\rho}_{i,j} = \sum_k^k \rho_{i,j}^k s_k w_k^2 \quad (\text{EQ 6})$$

where $\rho_{i,j}^k$ is formed from (EQ 5) for the k th pair, s_k equalizes the associated scaling of phase-to-height for the imaging geometry of pair k , and w_k^2 is an appropriate normalized weighting that can be used to accommodate data integrity based on signal-to-noise, etc.

This phase unwrapping solution includes the contributions of the multiple observations in a robust fashion, provides reduced sensitivity to model errors or phase errors introduced by bad observations, and offers, in general, better terrain elevation estimates

than can be obtained with any single pair of interferometric images.

For example, Figure 1 indicates what might depict a four-pass imaging scenario. With K independent images, there are at most $K - 1$ independent interferometric pairs for processing. Obviously, the Pass #1/Pass #4 pair have the largest effective baseline (greatest imaging geometry diversity) which offers the greatest height sensitivity and best height-to-phase-noise performance. However, overly steep terrain could induce regions of phase aliasing and destroy elevation information. The trick in exploiting this method lies in the selection of the pairwise observations to maximize independence and reduce the potential for phase aliasing.

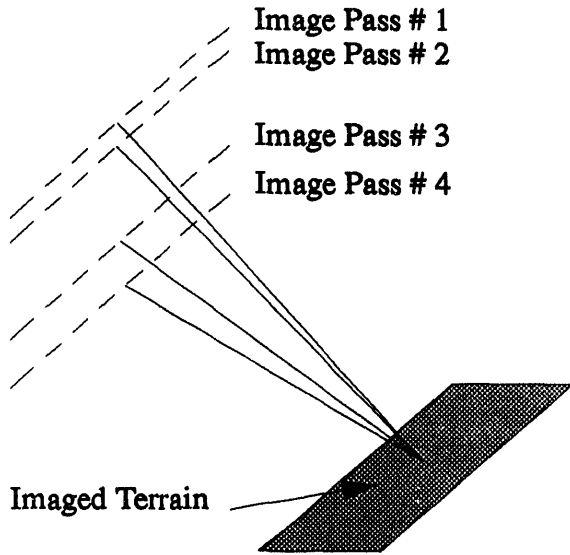


FIGURE 1. A Possible 4-pass Imaging Scenario.

3.0 Maximum Likelihood Multibaseline Method

The second class of methods for multibaseline terrain elevation estimation attacks the problem directly in a maximum likelihood (ML) formulation. For example, let the complex registered image at pixel l and SAR collection m be denoted by the model,

$$X_{l,m} = a_l \exp(j\omega_m h) + n_{l,m} \quad (\text{EQ 7})$$

where l denotes the pixel in an averaging box (i.e., $1 \leq l \leq L$; if the box is 4 by 4 then $L = 16$), m denotes the SAR collection number ($1 \leq m \leq M$), ω_m is a known constant and is a function of depression angle and radar center frequency, h denotes the terrain height and is assumed to be constant over the averaging box, $n_{l,m}$ is the additive noise term, and a_l denotes the complex scene reflectivity at pixel l . It is assumed that a_l and $n_{l,m}$ are complex gaussian random variables that are mutually independent over l and m . The respective variances are defined as: $E\{a_l^2\} = \sigma_a^2$, and $E\{n_{l,m}^2\} = \sigma_n^2$. By denoting $\tilde{a}_l = a_l \exp(j\omega_1 h)$, (EQ 7) can be simplified to yield the model,

$$X_{l,m} = \tilde{a}_l \exp(j(\omega_m - \omega_1) h) + n_{l,m}. \quad (\text{EQ 8})$$

Our objective is to derive a maximum likelihood (ML) estimator for the terrain height (denoted by \hat{h}_{ML}) given the observations indicated in (EQ 8). Let the vector \hat{x}_l denoting all M observations of pixel l be defined as,

$$\hat{x}_l = \tilde{a}_l \begin{bmatrix} 1 \\ e^{j(\omega_2 - \omega_1) h} \\ \dots \\ e^{j(\omega_M - \omega_1) h} \end{bmatrix} + \begin{bmatrix} n_{l,1} \\ n_{l,2} \\ \dots \\ n_{l,M} \end{bmatrix} = \tilde{a}_l \hat{V}_l + \hat{N}_l. \quad (\text{EQ 9})$$

Using the assumptions given above, the conditional probability of \hat{x}_l can be written as,

$$P(\hat{x}_l | h) = \frac{1}{\pi^M |Q|} \exp\{-\hat{x}_l^H Q^{-1} \hat{x}_l\} \quad (\text{EQ 10})$$

where $Q_l = E \{ \hat{x}_l^H \hat{x}_l \} = \sigma_a^2 \hat{V}_l \hat{V}_l^H + \sigma_n^2 I$. Since we have L independent pixel observations (which is the size of the averaging box), we can write the joint PDF as the product of the individual PDF's as follows,

$$P(\hat{\eta}|h) = \prod_{l=1}^L P(\hat{x}_l|h) = \frac{1}{\pi^{ML} |Q|^L} \exp \left\{ - \sum_{l=1}^L \hat{x}_l^H Q^{-1} \hat{x}_l \right\}, \quad (\text{EQ 11})$$

where $\hat{\eta}$ represents the vector of all $M \times L$ observations. The value of h that maximizes (EQ 11) can be shown to be the same h that maximizes the simplified expression,

$$P_1 = \sum_{l=1}^L \hat{x}_l^H \hat{V}_l \hat{V}_l^H \hat{x}_l = \sum_{l=1}^L |\hat{x}_l^H \hat{V}_l|^2. \quad (\text{EQ 12})$$

The function, $f(h) = \frac{1}{M} \sum_{m=1}^M |e^{j(\omega_m - \omega_1) h}|^2$,

derived from (EQ 12), called the *interferometer function*, defines the normalized response of an M element interferometer as a function of terrain height h . Potential height ambiguities (defined by the locations of the maxima) are depicted in Figure 2 for a typical 4-observation SAR collection.

The ML method offers potentially better performance than the unwrapping methods discussed previously, especially in regards to noise performance, measurement independence, and phase-to-height wrapping ambiguities. It is not without fault however. Initial experiments indicate difficulties when the observed data differ in some unknown way from the model assumptions. In other words, if the measurements do not fit the model, the ML method does not solve the correct problem.

In the corresponding poster session we provide several examples, containing actual and simulated SAR imagery, that illustrate the advantages and disadvantages of each method. It is hoped that these techniques help advance the utility of SAR interferometry in important civil applications.

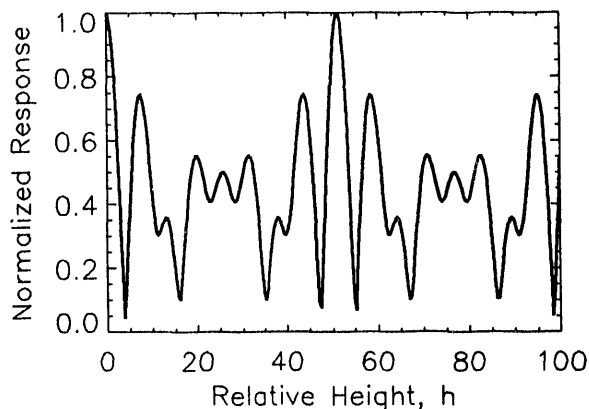


FIGURE 2. A Typical Interferometer Function for a 4-Observation SAR Collection.

This research was supported by the U.S. Department of Energy under contract DE-AC04-94AL85000.

References

- [1] L. C. Graham, "Synthetic interferometer radar for topographic mapping," Proc. IEEE, Vol. 62, no. 6, pp. 763-768, June 1974.
- [2] H. A. Zebker, and R. M. Goldstein, "Topographic mapping from interferometric synthetic aperture radar observations," J. Geophysical Res., Vol. 91, no. B5, pp. 4993-4999, April 10, 1986.
- [3] P. H. Eichel, D. C. Ghiglia, C. V. Jakowatz, Jr., P. A. Thompson, D. E. Wahl, "Spotlight SAR interferometry for terrain elevation mapping and interferometric change detection," submitted to IEEE Trans. AES.
- [4] D. C. Ghiglia and L. A. Romero, "Robust two-dimensional weighted and unweighted phase unwrapping that uses fast transforms and iterative methods," J. Opt. Soc. Am. A, Vol. 11, No. 1, pp. 107-117, January 1994.

DATE

FILMED

9 / 8 / 94

END

